



## Effect of dilution of fuel in CO<sub>2</sub> on the conversion of NH<sub>3</sub> to NO<sub>x</sub> during oxy-fuel combustion<sup>\*</sup>

Kun-zan QIU<sup>1</sup>, Ye YANG<sup>1</sup>, Zhuo YOU<sup>2</sup>, Zhi-hua WANG<sup>†‡1</sup>, Zhi-jun ZHOU<sup>1</sup>, Jun-hu ZHOU<sup>1</sup>, Ke-fa CEN<sup>1</sup>

<sup>(1)</sup>State Key Lab of Clean Energy Utilization, Zhejiang University, Hangzhou 310027, China

<sup>(2)</sup>Second Institute for Wuhan Ship Development & Design, Wuhan 430064, China

<sup>†</sup>E-mail: wangzh@zju.edu.cn

Received July 4, 2013; Revision accepted July 27, 2015; Crosschecked Sept. 15, 2015

**Abstract:** The indirect chemical effects of fuel dilution by CO<sub>2</sub> on NO formation were investigated numerically in this paper. CH<sub>4</sub> doped with NH<sub>3</sub> was used as fuel, while CO<sub>2</sub> and O<sub>2</sub> were mixed as oxidant. The dilution effect of CO<sub>2</sub> was then investigated through adding extra CO<sub>2</sub> to the reaction system. An isothermal plug flow reactor was used. An unbranched chain reaction mechanism is proposed to illustrate the chemical effects of CO<sub>2</sub> on the H/O/OH radical pool and NO<sub>x</sub>. Due to the reaction between CO<sub>2</sub> and H, extra NO will be formed in fuel-rich conditions, while NO will be inhibited in fuel-lean conditions and high CO<sub>2</sub> dilution conditions. The reaction affected the radical pools of OH, H, and O of the branched chain reaction, and then the formation and reduction of NO. The pool of H had the greatest effect on NO reduction. The results suggest that the indirect chemical effects on NO formation differ between diluted fuel oxy-fuel combustion conditions and normal oxy-fuel conditions.

**Key words:** CO<sub>2</sub>, Oxy-fuel combustion, NO, Fuel dilution

**doi:**10.1631/jzus.A1300231

**Document code:** A

**CLC number:** TQ534

### 1 Introduction

CO<sub>2</sub> is considered to be one of the most important anthropogenic gas emission species involved in global warming (Habib *et al.*, 2011). Oxy-fuel combustion is one of the advanced technologies used to capture CO<sub>2</sub> when burning fossil fuels (Buhre *et al.*, 2005). In oxy-fuel combustion, oxygen or a mixture of oxygen and flue gas, is used as an oxidizer instead of air. As a result, the volume fraction of CO<sub>2</sub> is much higher than that of typical air-fuel combustion conditions. With more than 95% concentrated in the product gas, through a series of rela-

tively simple purification processes, CO<sub>2</sub> can be compressed, transported, and stored (Buhre *et al.*, 2005).

Compared with typical air-fuel systems, the combustion process (as well as pollutant formation) will be different in the oxy-fuel combustion process due to the high CO<sub>2</sub> level (Chui *et al.*, 2003; Wang *et al.*, 2008). Undiluted, the temperature of oxy-fuel combustion will be much higher than that of air combustion because of the absence of nitrogen. To apply oxy-fuel combustion in ordinary boilers, flue gas needs to be recycled to maintain the temperature at an acceptable level (Chui *et al.*, 2004). The flame temperature decreases when the amount of oxygen in the inlet is reduced and the amount of recycled flue gas is increased (Bhuiyan and Naser, 2015a). The temperature profile in the boiler may be changed due to the differences in heat capacity between CO<sub>2</sub> and N<sub>2</sub>. The flame propagation speed also differs (Normann *et al.*, 2009) due to differences in heat capacity

<sup>‡</sup> Corresponding author

<sup>\*</sup> Project supported by the National Basic Research Program (973 Program) of China (No. 2012CB214906)

ORCID: Kun-zan QIU, <http://orcid.org/0000-0003-0978-2697>; Zhi-hua WANG, <http://orcid.org/0000-0002-7521-2900>

© Zhejiang University and Springer-Verlag Berlin Heidelberg 2015

and chemical properties between CO<sub>2</sub> and N<sub>2</sub>. Significant variation has been found in the temperature distribution and CO<sub>2</sub> concentration when comparing air-firing with oxy-firing under different recycling ratios in a computational model of co-firing of biomass with coal under oxy-fuel conditions (Bhuiyan and Naser, 2015b).

The reduction of NO<sub>x</sub> due to recycled flue gas is a known benefit of oxy-fuel combustion (Kiga *et al.*, 1997; Chui *et al.*, 2004; Buhre *et al.*, 2005; Ahn *et al.*, 2009). Part of the NO in the flue gas is reduced by precursors, such as HCN and NH<sub>3</sub>, and carbonaceous reducing radicals in fuel-rich regions (Buhre *et al.*, 2005).

However, the formation of NO<sub>x</sub> during combustion will be indirectly affected by the occurrence of high concentrations of carbon dioxide. As is well known, the production of NO<sub>x</sub> can be dramatically reduced through staging combustion technology, even without flue gas recirculation (Boushaki *et al.*, 2008; 2009). Much more NO<sub>x</sub> reduction can be achieved by staging compared with the air-fuel combustion process (Cao *et al.*, 2010; Watanabe *et al.*, 2011). Also, thermal NO<sub>x</sub> would be dramatically reduced because of the absence of nitrogen from the system (Normann *et al.*, 2008).

CO<sub>2</sub> is not 100% chemically inert (Hecht *et al.*, 2011), although it is usually the final combustion product of elemental carbon. Reaction (1) illustrates how OH is formed from CO<sub>2</sub> and H (Glarborg and Bentzen, 2008; Mendiara and Glarborg, 2009; Watanabe *et al.*, 2011). A chain carrier of H of a branched chain reaction during combustion of fuels with H is involved in this reaction (Fig. 1). The pathways from nitrogen containing species to NO<sub>x</sub> are linked closely to chain carriers. The formation of NO<sub>x</sub>, fuel NO, is then affected indirectly by the chemical effect of CO<sub>2</sub>. The effect of oxy-fuel combustion on NO formation is also directly increased by high CO<sub>2</sub> concentrations through Reaction (2), which is also believed to be the reason for the CO<sub>2</sub> chemical effect on NO (Feng *et al.*, 1998).



Mendiara and Glarborg (2009) studied the oxidation of methane and ammonia under highly di-

luted conditions in CO<sub>2</sub> and N<sub>2</sub> via experiment and numerical simulation. They found that, compared with nitrogen-diluted conditions, CO<sub>2</sub> facilitates NO formation under fuel-rich conditions but inhibits it under fuel-lean or stoichiometric conditions. It is believed that high levels of CO<sub>2</sub> facilitate the formation of NO by increasing the OH/H ratio. Furthermore, the formation of HNCO through NH<sub>2</sub>+CO is increased due to high CO levels. However, some reactions of N containing species with O or H are inhibited due to decreased concentrations of O and H, such as NH<sub>2</sub>+O to form HNO and NH<sub>2</sub>+H to form NH. These two reactions are important pathways for NH<sub>3</sub> to form NO, especially NH<sub>2</sub>+O to form HNO.

In a study of staged oxy-fuel combustion, Watanabe and Ichiro *et al.* (2011) observed higher OH levels via planar laser induced fluorescence (PLIF) in a fuel/O<sub>2</sub>/CO<sub>2</sub> flame than in a fuel/air flame at an O<sub>2</sub>/CH<sub>4</sub> ratio of 0.7 (equivalence ratio of 1.42). They believed that Reaction (1) does not compete with the branched chain reaction for the H atom since the radical pool of chain carriers is large. The oxidation of species containing nitrogen increases due to the increased OH radicals, and NO<sub>x</sub> tends to be reduced in fuel-rich conditions. Because precursors of NO<sub>x</sub> are prevented from being oxidized by supplementary oxygen in the secondary stream, staged combustion in oxy-fuel combustion performs better than air-fuel combustion in reducing nitrogen oxidation.

We conclude that, apart from the equivalence ratio under high levels of CO<sub>2</sub>, the formation of NO<sub>x</sub> may be affected by the level of fuel in the mixture. But little is known about how variation in the level of fuel affects NO<sub>x</sub> formation in an O<sub>2</sub>/CO<sub>2</sub> atmosphere. The fuel level limits the speed of the branched chain reaction.

In this study, variation in the chemical effects of CO<sub>2</sub> on NO<sub>x</sub> formation from NH<sub>3</sub> due to changes in the fuel level in mixtures with high CO<sub>2</sub> concentrations was investigated via numerical simulation.

## 2 Methods

Combustion of CO<sub>2</sub> diluted CH<sub>4</sub>/NH<sub>3</sub> fuel with O<sub>2</sub>/CO<sub>2</sub> as an oxidizer was simulated using a Chemkin Pro plug flow reactor. The reactor was 90 cm long and 26 mm in diameter, and was set in the

isothermal range of 1073–1773 K. The inlet velocity was set to 30 cm/s. The initial temperature of the mixture was set to the same temperature as that of the reactor to maintain a residence time of 3 s, which is similar to that found in boilers in thermal plants burning pulverized coal.

The composition of the mixtures is listed in Table 1. The simulated fuel streams were doped with NH<sub>3</sub> as the NO<sub>x</sub> precursor in volatiles from coal. The volume fraction of NH<sub>3</sub> was set to 2% of the total CH<sub>4</sub> fuel stream according to the ratio of N to C of lignite from Yunnan Province in China. O<sub>2</sub> occupied 21% of the volume of the O<sub>2</sub>/CO<sub>2</sub> oxidizer. The equivalence ratios of the mixture of CH<sub>4</sub>/NH<sub>3</sub> and O<sub>2</sub>/CO<sub>2</sub> were 0.6, 1.05, and 1.5 in Cases A1, A2, and A3, respectively. Each mixture in group A was diluted 10 times with CO<sub>2</sub> in group B and 100 times in group C.

The numerical simulation was carried out using Chemkin Pro commercial software. Two reaction mechanisms were adopted: the GRI-Mech mechanism 3.0 (GRI30), and the mechanism developed by Mendiara and Glarborg (2009), referred to as M09 in this study. To study the effect of Reaction (1), the cases in Table 1 were also simulated with mechanisms without Reaction (1), namely the reverse reaction of CO+OH to form H+CO<sub>2</sub>. These mechanisms are referred to as IRGRI and IRM09.

The conversion ratio from NH<sub>3</sub> to exhaust NO<sub>x</sub> (NO<sub>x</sub> CR) was defined as:

$$\text{NO}_x \text{ CR} = \frac{\text{Exhaust NO}_x \text{ flow rate}}{\text{Inflow NO}_x \text{ flow rate}}$$

### 3 Results and discussion

An unbranched chain reaction mechanism is proposed to illustrate the chemical effect of CO<sub>2</sub> on the radical pool (Fig. 1). The reactions CO<sub>2</sub>+H to form OH and CO, OH+H<sub>2</sub> to form H<sub>2</sub>O and H can be taken as chain reactions without branching. The availability of O/H/OH, as well as the oxidation and reduction of N-containing species, can be affected by the relative dominance of the two types of chain reaction.

Results from the GRI30 and M09 mechanisms (Fig. 2) show coherence to a certain extent in predicting the conversion ratio of nitrogen element in methane flame to NO<sub>x</sub> (NO<sub>x</sub> conversion ratio) in an undiluted O<sub>2</sub>/CO<sub>2</sub> atmosphere (Watanabe *et al.*, 2011) and in simulating NH<sub>3</sub> oxidation in an O<sub>2</sub>/CO<sub>2</sub> atmosphere with diluted CH<sub>4</sub> as fuel (Mendiara and

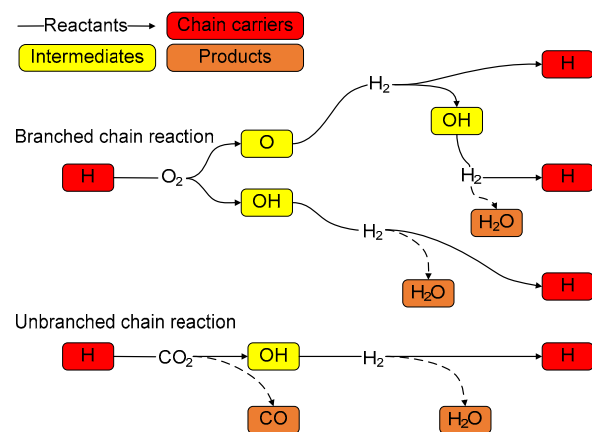


Fig. 1 Branched/Unbranched chain reactions in oxy-fuel combustion

Table 1 Gas composition at the inlet of the reactor

Case name	Gas composition (% in volume)				Equivalence ratio, $\phi$	Mechanism calculated
	CH <sub>4</sub>	NH <sub>3</sub>	O <sub>2</sub>	CO <sub>2</sub>		
A1	5.88	0.1176	19.74	74.26	0.6	GRI30, IRGRI
A2	9.84	0.1969	18.89	71.07	1.05	
A3	13.48	0.2697	18.11	68.14	1.5	
B1	0.59	0.0118	1.97	97.43	0.6	GRI30, IRGRI
B2	0.98	0.0197	1.89	97.11	1.05	
B3	1.35	0.0270	1.81	96.81	1.5	
C1	0.06	0.0012	0.20	99.74	0.6	M09, IRM09
C2	0.098	0.0020	0.19	99.71	1.05	
C3	0.13	0.0027	0.18	99.68	1.5	

Glarborg, 2009), and both mechanisms performed very well. The M09 mechanism was a little better than GRI30 in the latter simulation. Thus, simulated results for conditions in groups A and C were used only for mechanisms based on GRI30 and M09, respectively. The effects of Reaction (1) for NH<sub>3</sub> oxidation in group B simulated by GRI30 and M09 were similar, so only results from GRI30 were used in this study.

Figs. 3–5 compare the conversion ratios of NH<sub>3</sub> to NO<sub>x</sub> at the end of the plug flow reactors using both mechanisms, under fuel-rich, stoichiometric, and fuel-lean conditions, respectively.

Fig. 3 shows the results for fuel-rich conditions. The NO<sub>x</sub> conversion ratio remained very low under undiluted and fuel-rich conditions (A3). NO<sub>x</sub> formation was increased by Reaction (1) under A3 and B3 conditions. For C3 conditions, NO<sub>x</sub> formation was inhibited at temperatures between 1273 K and 1373 K, and increased above 1573 K.

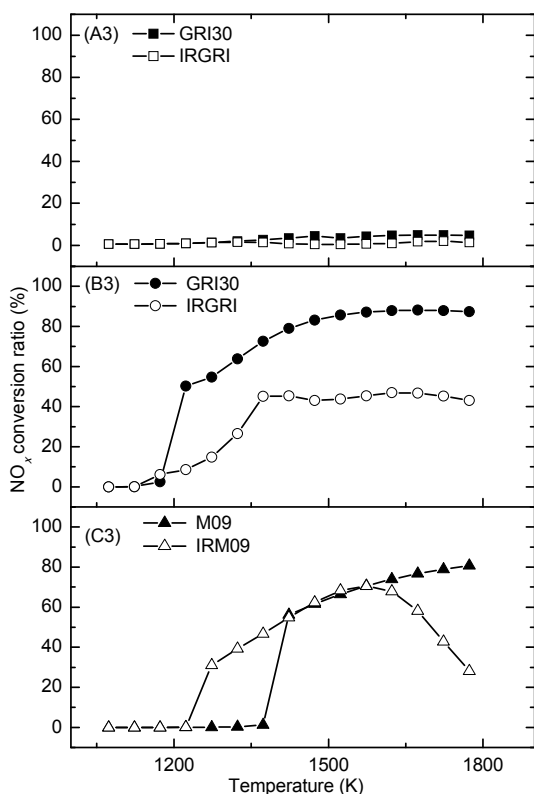


Fig. 3 Conversion ratio of N to NO<sub>x</sub> at the end of the reactor vs. temperature under fuel-rich conditions ( $\Phi=1.5$ ; A3, B3, and C3 correspond to conditions described in Table 1)

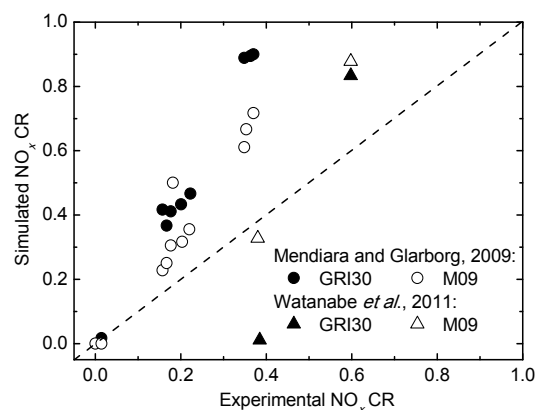


Fig. 2 Comparison of simulated values of NO<sub>x</sub> conversion ratio (CR) with experimental values from Watanabe et al. (2011) and Mendiara and Glarborg (2009) (Circles denote conditions with CO<sub>2</sub> levels of about 90% and diluted fuel; triangles denote conditions with about 70% CO<sub>2</sub>; the values calculated using the GRI mechanism are shown as closed symbols while those calculated using the M09 mechanism are shown by open symbols)

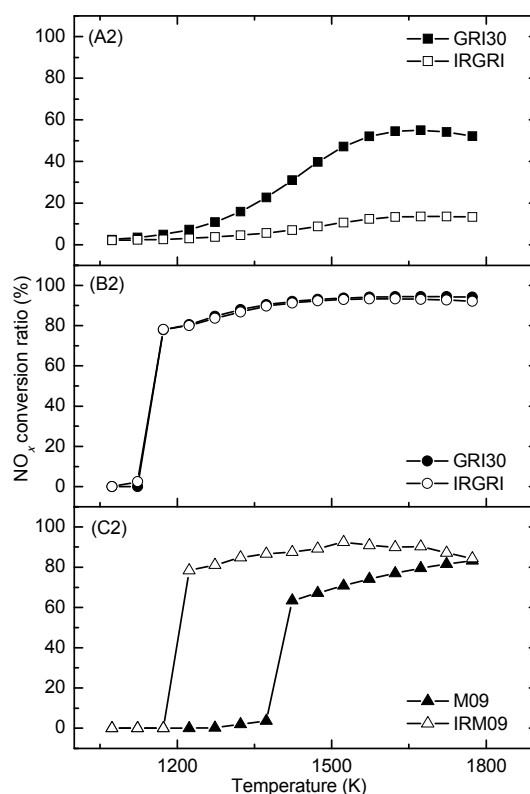


Fig. 4 Conversion ratio of N to NO<sub>x</sub> at the end of the reactor vs. temperature under stoichiometric conditions ( $\Phi=1.05$ ; A2, B2, and C2 correspond to conditions described in Table 1)

Fig. 4 shows the results for stoichiometric conditions. The  $\text{NO}_x$  conversion ratio increased as the temperature increased. The conversion ratios of  $\text{NO}_x$  from the mechanisms were nearly the same under 10 times dilution conditions. Reactions to form  $\text{NO}$  were facilitated without  $\text{CO}_2$  dilution, but inhibited under 100 times  $\text{CO}_2$  dilution conditions.

Fig. 5 shows the results for fuel-lean conditions.  $\text{NO}_x$  formation was inhibited regardless of dilution, and the effect increased with  $\text{CO}_2$  dilution.

We can conclude from Figs. 3–5 that the chemical effect of  $\text{CO}_2$  on the conversion of  $\text{NH}_3$  to  $\text{NO}$  through Reaction (1) is impacted by both the equivalence ratio and  $\text{CO}_2$  level.  $\text{NO}$  formation is facilitated under fuel-rich conditions with undiluted oxy-fuel  $\text{CO}_2$  concentrations, but is inhibited under fuel-lean conditions and very high  $\text{CO}_2$  concentrations. When the inlet mixture was over 99%  $\text{CO}_2$ , the reaction of  $\text{CO}_2 + \text{H}$  to form  $\text{CO}$  and  $\text{OH}$  led to a reduced conversion ratio of  $\text{NH}_3$  to  $\text{NO}$ , under all equivalence ratios.  $\text{NO}$  formation was slightly

increased (or decreased) under near stoichiometric (or fuel-lean) conditions.

Fig. 6 shows the volume fractions of  $\text{NO}$  along the axis of the reactor at 1523 K, and equivalence ratios of 0.6, 1.05, and 1.5 without inlet  $\text{CO}_2$  dilution.  $\text{NO}$  is first produced in the reactor, and then part of the  $\text{NO}$  is reduced along the reactor under fuel-rich and stoichiometric conditions. Formation is facilitated under fuel-rich conditions due to Reaction (1), and  $\text{NO}$  destruction is inhibited due to Reaction (1) under fuel-rich and stoichiometric conditions, while  $\text{NO}$  is gradually reduced. The conversion ratio of  $\text{NO}$  was slightly higher when Reaction (1) was applied to the mechanism. There were no significant differences in the peak volume fraction of  $\text{NO}$  between the results from the two mechanisms under fuel-lean and stoichiometric conditions.  $\text{NO}$  is gradually reduced under stoichiometric conditions and this process was inhibited due to Reaction (1), while  $\text{NO}$  is not reduced under fuel-lean conditions. The trends of the  $\text{NO}$  volume fraction along the reactor

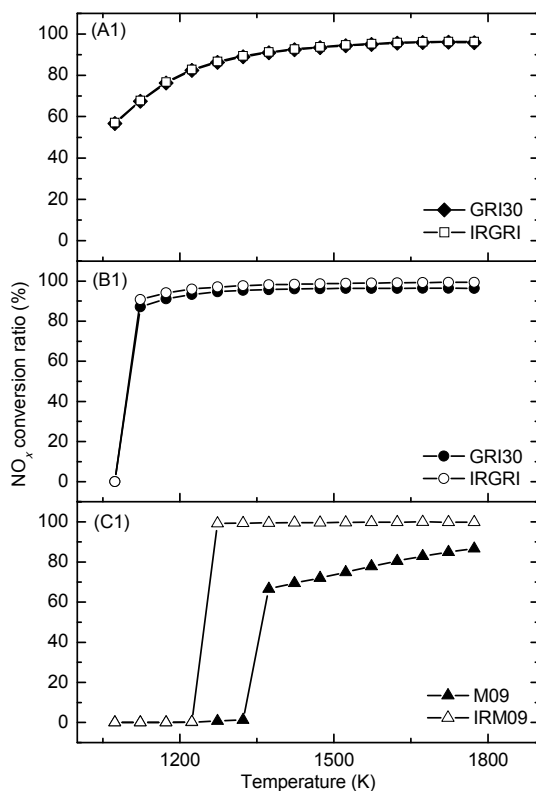


Fig. 5  $\text{NO}_x$  conversion ratio at the end of the reactor vs. temperature under fuel-lean conditions ( $\phi=0.6$ ; A1, B1, and C1 correspond to conditions described in Table 1)

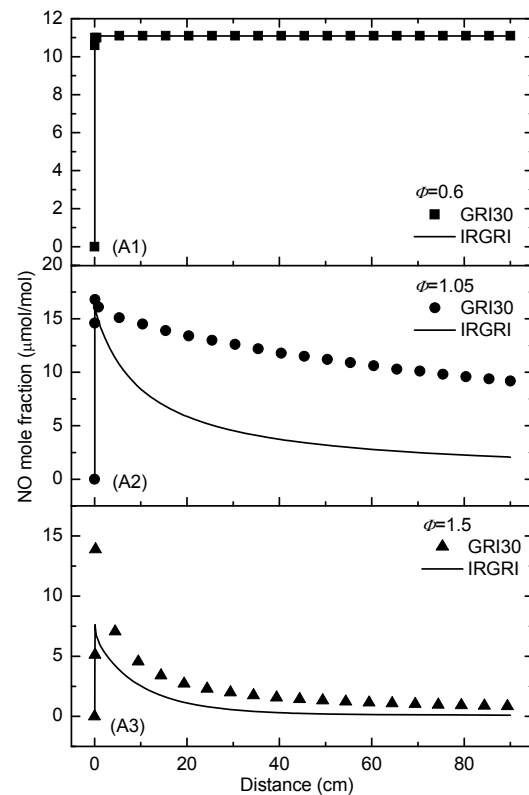


Fig. 6 Profile of  $\text{NO}$  along the reactor under conditions A1, A2, and A3 at  $T=1523$  K (A1, A2, and A3 correspond to conditions described in Table 1)

at 1523 K are similar to those shown in Fig. 6 (A2) under condition B3 (fuel-rich), and similar to those shown in Fig. 6 (A1) under conditions B1 (fuel-lean) and B2 (near stoichiometric).

Fig. 7 shows mole fractions of radicals OH and H along the axis of the reactor at 1523 K, and equivalence ratios of 0.6, 1.05, and 1.5 without inlet CO<sub>2</sub> dilution. The concentration of H was not always reduced by the reaction of CO<sub>2</sub>+H forming CO and OH. This result differs from that found by Mendiara and Glarborg (2009). As with the fuel-rich case, more OH and H were produced due to this reaction, while less H was produced under near stoichiometric conditions. H and OH are important intermediate species for the conversion of NH<sub>3</sub> to NO, though the paths may differ under fuel-rich and stoichiometric conditions. Under fuel-rich conditions, the increase in OH and H resulted in a higher peak of NO, while under near stoichiometric conditions, Reaction (1) resulted in more OH but less H. The effect on the

peak value of NO and its reduction after the peak was then weakened compared with the effects under fuel-rich conditions.

Fig. 8 shows the main pathways through which NO was reduced to N<sub>2</sub> after its peak. The main path was NO+H to form HNO (Reaction (3)), then HNO was reduced to NH by CO and H<sub>2</sub> (Reactions (4) and (5)). At the same time, HNO was reduced to NO by H (Reaction (6)) and NO was reduced to N<sub>2</sub>O by NH (Reaction (7)), and at the end N<sub>2</sub>O was reduced to N<sub>2</sub> by H (Reaction (8)) and M (Reaction (9)). In an inferior path, NO was directly reduced to N<sub>2</sub> by NH (Reaction (10)) and N. The availability of H is the major reason for the change in the reaction rate of NO reduction induced by changing the existence of Reaction (1). Reactions (3) and (8) from NO to HNO were facilitated by the increased level of H, resulting in a greater formation of NH. Hence, the reactions from NO to N<sub>2</sub>O and N<sub>2</sub>, and the reaction from N<sub>2</sub>O to N<sub>2</sub>, were facilitated.

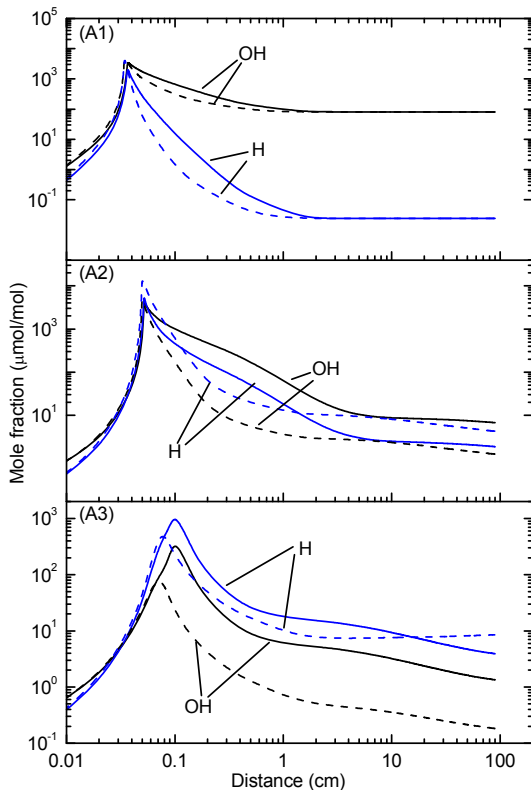


**Fig. 7 Profile of OH and H radicals along the reactor under conditions A1, A2, and A3 at T=1523 K. Solid lines denote the GRI30 mechanism, while dashed lines denote the IRGRI mechanism. A1, A2, and A3 correspond to conditions described in Table 1**

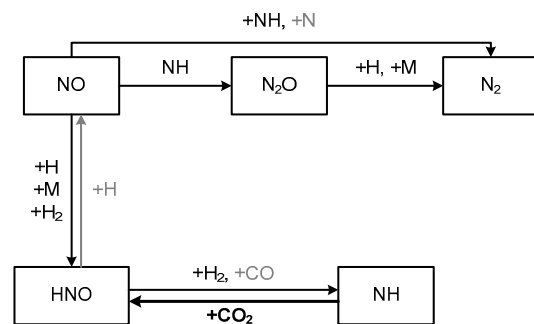
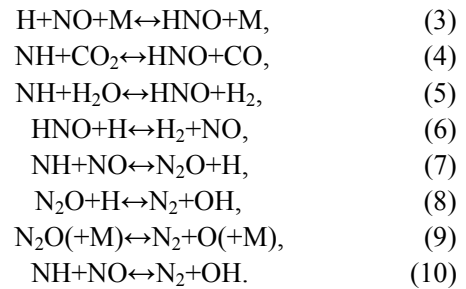


**Fig. 8 Main reaction path for NO reduction (the bolded one is for GRI30 only, and the grey ones are for IRGRI only)**

The reaction CO<sub>2</sub>+H to form OH and CO resulted in a higher H level at the peak NO concentration and eliminated the consumption of H during NO reduction after the peak. The higher H level was the

main factor contributing to the reduction of NO under conditions without CO<sub>2</sub> dilution. In a reducing atmosphere, the reduction of NO was facilitated due to the higher H level resulting from Reaction (1). Lower H levels were obtained under stoichiometric conditions. Under lean conditions, NO would not be reduced once it has been produced in the reaction zone.

Fig. 9 shows the volume fraction of NO along the reactor at 1523 K, 100 times CO<sub>2</sub> dilution, and an equivalence ratio of 1.05. The curves with an equivalence ratio of 0.6 and 1.5 are similar to those shown in Fig. 9. This shows that the formation of NO is inhibited due to Reaction (1) regardless of the equivalence ratio, once the reactant is diluted 100 times in CO<sub>2</sub>. Also, under these conditions none of the NO formed is reduced after it has reached its maximum concentration. The start of NO formation is delayed due to Reaction (1). With a high degree of dilution in CO<sub>2</sub>, concentrations of all the species are low, except for CO<sub>2</sub>. The H radical tends to be caught and consumed by CO<sub>2</sub>, so the reaction is led by the unbranched chain reaction in the initial stage of the reaction. The branched chain reactions become important only when active chain carriers of H are accumulated at sufficiently high levels. With the IRGRI mechanism, the branched chain reactions lead the reaction at the beginning. The delay of the branched chain reaction results in reduced H, O, and OH levels, which are vital to the oxidation of nitrogen species to NO. Therefore, the formation of NO decreases due to the chemical effect of CO<sub>2</sub>. NO is not reduced even after its peak under high CO<sub>2</sub> dilution fuel-rich conditions because of low H availability in the reaction zone.

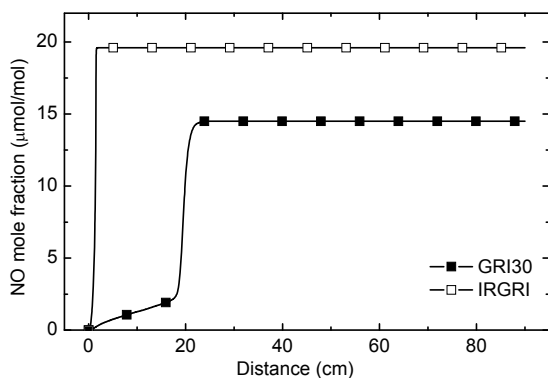


Fig. 9 Profile of NO along the reactor under condition C2 at  $T=1523$  K

Table 2 shows the indirect effect of Reaction (1) on the formation and reduction of NO in terms of the conversion ratio. The promotion effect of Reaction (1) on NO during the formation period is weakened gradually with CO<sub>2</sub> dilution. NO formation is inhibited under high CO<sub>2</sub> dilution and fuel-lean conditions by Reaction (1) indirectly (Fig. 9). The trends of the indirect effect of CO<sub>2</sub> dilution on NO reduction are similar to those on NO formation. But under high dilution conditions, regardless of the equivalence ratio, the promotion effect on NO reduction resulting from Reaction (1) dissipates. Under the condition of 100 times CO<sub>2</sub> dilution, Reaction (1) has no effect on the reduction process of NO.

Table 2 Effect of Reaction (1) on formation and reduction of NO at  $T=1523$  K

Equivalence ratio	Item	Effect value ( $\mu\text{mol/mol}$ )		
		A	B	C
0.6	Formation <sup>a</sup>	-0.3	-2.5	-21.9
	Reduction <sup>b</sup>	0.0	0.0	-0.1
1.05	Formation	0.2	-2.8	-23.1
	Reduction	-36.4	-3.6	-1.4
1.5	Formation	28.8	-1.1	-26.9
	Reduction	25.8	-43.0	-8.9

<sup>a</sup> Comparison of the peak values of NO along the reactor between the full mechanisms (GRI30 or M09) and the artificial mechanisms (IRGRI or IRM09); a positive value means formation of NO is facilitated by Reaction (1); a negative value means formation of NO is inhibited by Reaction (1); <sup>b</sup> comparison of the concentration difference (peak (NO) and end (NO)) along the reactor between the full mechanisms (GRI30 or M09) and the artificial mechanisms (IRGRI or IRM09); a positive value means reduction of NO after the peak is facilitated by Reaction (1); a negative value means reduction of NO after the peak is inhibited by Reaction (1)

Under fuel-rich conditions without CO<sub>2</sub> dilution, NO is rapidly produced and then most of it is subsequently reduced. The conversion from NH<sub>3</sub> to NO is facilitated due to the increased radical pool resulting from Reaction (1). On the other hand, the process of reduction of NO to N<sub>2</sub> relies on the residual radical pool of O/H/OH after the NO peak, especially the pool of H. These two opposite effects result in only a slight change to the NO conversion rate at the end of the reaction. Under the conditions with 10 times CO<sub>2</sub> dilution, the branched chain reactions are weakened, and the radical pool is eliminated. The influence of Reaction (1) on the radical pool is then weakened and the increase in NO is reduced. After the peak of

NO, the consumption of H due to Reaction (1) inhibits the reduction of NO, which results in a higher  $\text{NO}_x$  concentration at the end of the reaction. Under conditions with even higher  $\text{CO}_2$  dilution, the increase in  $\text{NO}_x$  formation is even smaller, and because of the lower level of reactants, the relative concentration of H at the peak of NO is lower. NO is hardly reduced after the peak. So at the end of the reaction, the level of NO is higher when Reaction (1) is adopted in the mechanism.

Under stoichiometric conditions, NO formation before its peak is slightly facilitated without  $\text{CO}_2$  dilution due to Reaction (1). As the dilution with  $\text{CO}_2$  increases, this effect on NO is severely inhibited and the reduction effect gradually weakens (Table 2). The indirect effects of Reaction (1) on the  $\text{NO}_x$  conversion ratio at the end of the reaction are changed from facilitating without  $\text{CO}_2$  dilution, to insignificant with 10 times  $\text{CO}_2$  dilution, and then to inhibition with 100 times  $\text{CO}_2$  dilution.

Under fuel-lean conditions, formation of NO is inhibited by Reaction (1) regardless of the extent of dilution with  $\text{CO}_2$ . NO formed is not reduced under fuel-lean conditions.

Fig. 10 shows the ratio of residual  $\text{NH}_3$  at the end of the reaction under fuel-rich conditions at different temperatures. There are temperature ranges where the conversion of  $\text{NH}_3$  is initiated but not completed. In these temperature regions, the conversion of  $\text{NH}_3$  in the plug flow reactor simulated with the M09 mechanism is slower than that with the IRM09 mechanisms, under conditions of 100 times  $\text{CO}_2$  dilution. Simulations with GRI30 and IRGRI yield the same conclusion. Under conditions of 10 times dilution, the conversion of  $\text{NH}_3$  is faster with the GRI30 mechanism. The conversion of ammonia under fuel-rich conditions is a process in which H atoms are gradually lost. The N-H bonds are attacked by active radicals such as O, H, and OH. As described above, the radical pool of O/H/OH is affected by Reaction (1) and the effects differ with different  $\text{CO}_2$  dilution times. The  $\text{NH}_3$  conversion is faster with a denser radical pool. The role of Reaction (1) becomes more important as the dilution with  $\text{CO}_2$  increases. The weakening of the branched chain reaction results in relatively light radical pools, and the conversion of  $\text{NH}_3$  is consequently inhibited.

Fig. 11 shows the  $\text{NH}_3$  residual ratio at the end of the reaction at different temperatures under fuel-

lean conditions. The conversion of  $\text{NH}_3$  is inhibited due to the existence of Reaction (1) under conditions with 100 times  $\text{CO}_2$  dilution. Under conditions with 10 times  $\text{CO}_2$  dilution or no dilution, the conversion of  $\text{NH}_3$  is not influenced by the absence of Reaction (1) in the mechanism. The results are similar under conditions with an equivalence ratio of 1.05. Under conditions with 10 times  $\text{CO}_2$  dilution or no dilution, H in the reaction space is consumed rapidly by the branched chain reaction. The influence of the reaction on the radical pool and the whole reaction space is then limited. Therefore, Reaction (1) has almost no influence on  $\text{NH}_3$  conversion. Under conditions with 100 times  $\text{CO}_2$  dilution, the dominance of the branched chain reaction diminishes and the radical pools decrease. The conversion of  $\text{NH}_3$  is then inhibited (Fig. 10).

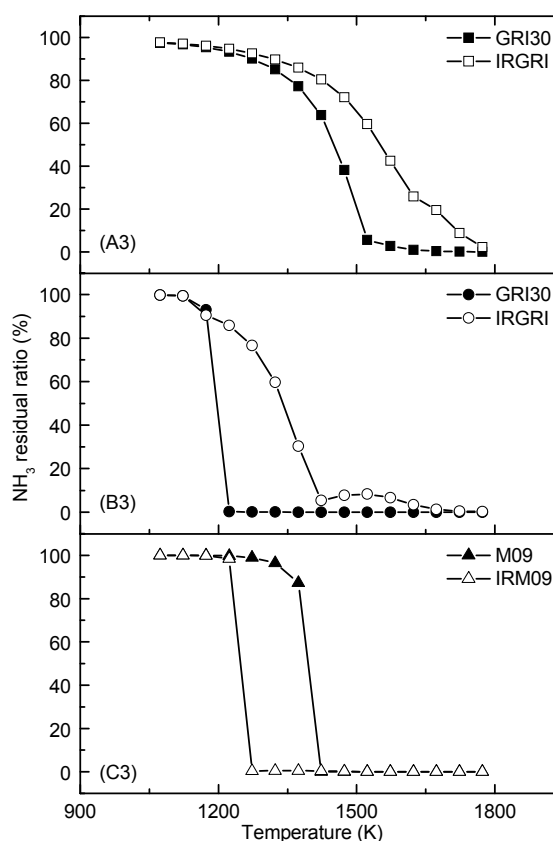


Fig. 10 Residual ratio of  $\text{NH}_3$  at the end of the reactor under fuel-rich conditions ( $\Phi=1.5$ ; A3, B3, and C3 correspond to conditions described in Table 1)

Fig. 12 shows the conversion ratio of nitrogen to main products at the end of the reaction under an

equivalence ratio of 1.5 with 10 times CO<sub>2</sub> dilution. The final products of nitrogen comprise mainly N<sub>2</sub> and NO<sub>x</sub>. N<sub>2</sub>O and HNCO would be formed under relatively low temperatures, between 1100 K and 1400 K. N<sub>2</sub>O tended to be produced under conditions of low temperatures, low equivalence ratios, and high CO<sub>2</sub> dilution levels, while HNCO was produced at low temperatures and high CO<sub>2</sub> dilution levels. The chemical effect of CO<sub>2</sub> played a more important role on HNCO than on N<sub>2</sub>O. Formation of HNCO was facilitated due to the chemical effect.

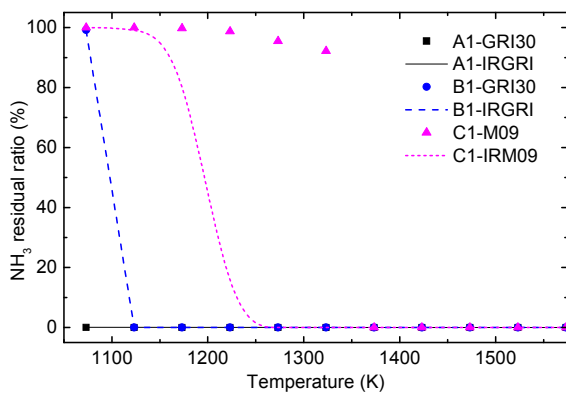


Fig. 11 Residual ratio of NH<sub>3</sub> at the end of the reactor under fuel-lean conditions ( $\Phi=0.6$ )

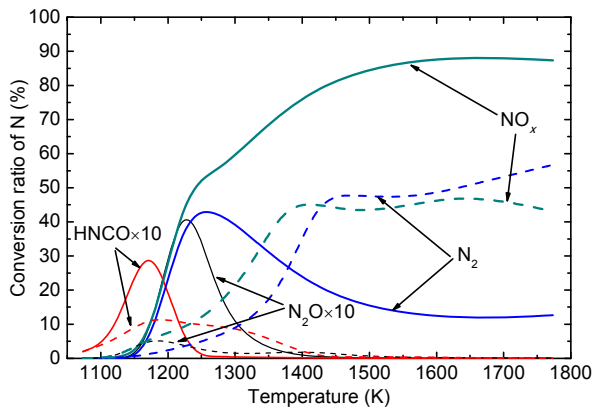


Fig. 12 Conversion ratio of nitrogen to main products in condition B3 ( $\Phi=1.5$ , solid lines denote the GRI30 mechanism, while dashed lines denote the IRGRI mechanism)

## 4 Conclusions

In this paper, the indirect relationship between the fuel level in mixtures of high CO<sub>2</sub> level and the

effect of CO<sub>2</sub> via the reaction CO<sub>2</sub>+H to form OH and CO on NO<sub>x</sub> formation from NH<sub>3</sub> were studied through numerical simulation.

Generally, the reaction CO<sub>2</sub>+H→CO+OH facilitates NO formation under fuel-rich conditions without CO<sub>2</sub> dilution, but inhibits NO formation under fuel-lean conditions with high CO<sub>2</sub> dilution. The radical pool of the chain carriers O/H/OH is affected, thereby influencing the formation and reduction of NO. The reduction of NO is affected mostly by H.

An unbranched chain reaction mechanism was proposed to illustrate the chemical effect of CO<sub>2</sub> on the radical pool and NO<sub>x</sub> formation and reduction.

As the CO<sub>2</sub> concentration increases, the mutual promotion of the unbranched chain reaction and the branched reaction gradually changes to mutual competition for H, which gradually weakens the promotion of NO formation. Under conditions with CO<sub>2</sub> levels higher than 90%, however, the formation of NO is inhibited.

The competition for H as CO<sub>2</sub> concentration increases influences the conversion of NH<sub>3</sub>, changing from facilitation to inhibition of NH<sub>3</sub> conversion under fuel-rich conditions, and from no influence to inhibiting conversion under near stoichiometric and fuel-lean conditions.

## References

- Ahn, J., Kim, H.J., Choi, K.S., 2009. Combustion characteristics of oxy-fuel burners for CO<sub>2</sub> capturing boilers. *Journal of Thermal Science and Technology*, **4**(3):408-413. [doi:10.1299/jtst.4.408]
- Bhuiyan, A.A., Naser, J., 2015a. Numerical modelling of oxy fuel combustion, the effect of radiative and convective heat transfer and burnout. *Fuel*, **139**:268-284. [doi:10.1016/j.fuel.2014.08.034]
- Bhuiyan, A.A., Naser, J., 2015b. Computational modelling of co-firing of biomass with coal under oxy-fuel condition in a small scale furnace. *Fuel*, **143**:455-466. [doi:10.1016/j.fuel.2014.11.089]
- Boushaki, T., Mergheni, M.A., Sautet, J.C., et al., 2008. Effects of inclined jets on turbulent oxy-flame characteristics in a triple jet burner. *Experimental Thermal and Fluid Science*, **32**(7):1363-1370. [doi:10.1016/j.expthermflusc.2007.11.009]
- Boushaki, T., Sautet, J.C., Labegorre, B., 2009. Control of flames by tangential jet actuators in oxy-fuel burners. *Combustion and Flame*, **156**(11):2043-2055. [doi:10.1016/j.combustflame.2009.06.013]
- Buhre, B.J.P., Elliott, L.K., Sheng, C.D., et al., 2005. Oxy-fuel combustion technology for coal-fired power generation. *Progress in Energy and Combustion Science*, **31**(4):

- 283-307. [doi:10.1016/j.peccs.2005.07.001]
- Cao, H., Sun, S., Liu, Y., et al., 2010. Computational fluid dynamics modeling of NO<sub>x</sub> reduction mechanism in oxy-fuel combustion. *Energy & Fuels*, **24**(1):131-135. [doi:10.1021/ef900524b]
- Chui, E.H., Douglas, M.A., Tan, Y.W., 2003. Modeling of oxy-fuel combustion for a western Canadian sub-bituminous coal. *Fuel*, **82**(10):1201-1210. [doi:10.1016/S0016-2361(02)00400-3]
- Chui, E.H., Majeski, A.J., Douglas, M.A., et al., 2004. Numerical investigation of oxy-coal combustion to evaluate burner and combustor design concepts. *Energy*, **29**(9-10):1285-1296. [doi:10.1016/j.energy.2004.03.102]
- Feng, B., Ando, T., Okazaki, K., 1998. NO destruction and regeneration in CO<sub>2</sub> enriched CH<sub>4</sub> flame. *JSME International Journal Series B-Fluids and Thermal Engineering*, **41**(4):959-965. [doi:10.1299/jsmeb.41.959]
- Glarborg, P., Bentzen, L.L.B., 2008. Chemical effects of a high CO<sub>2</sub> concentration in oxy-fuel combustion of methane. *Energy & Fuels*, **22**(1):291-296. [doi:10.1021/ef7005854]
- Habib, M.A., Badr, H.M., Ahmed, S.F., et al., 2011. A review of recent developments in carbon capture utilizing oxy-fuel combustion in conventional and ion transport membrane systems. *International Journal of Energy Research*, **35**(9):741-764. [doi:10.1002/er.1798]
- Hecht, E.S., Shaddix, C.R., Molina, A., et al., 2011. Effect of CO<sub>2</sub> gasification reaction on oxy-combustion of pulverized coal char. *Proceedings of the Combustion Institute*, **33**(2):1699-1706. [doi:10.1016/j.proci.2010.07.087]
- Kiga, T., Takano, S., Kimura, N., et al., 1997. Characteristics of pulverized-coal combustion in the system of oxygen recycled flue gas combustion. *Energy Conversion and Management*, **38**:S129-S134. [doi:10.1016/S0196-8904(96)00258-0]
- Mendiara, T., Glarborg, P., 2009. Ammonia chemistry in oxy-fuel combustion of methane. *Combustion and Flame*, **156**(10):1937-1949. [doi:10.1016/j.combustflame.2009.07.006]
- Normann, F., Andersson, K., Leckner, B., et al., 2008. High-temperature reduction of nitrogen oxides in oxy-fuel combustion. *Fuel*, **87**(17-18):3579-3585. [doi:10.1016/j.fuel.2008.06.013]
- Normann, F., Andersson, K., Leckner, B., et al., 2009. Utilization of reburn reactions for NO<sub>x</sub> control in oxy-fuel combustion. AICHE Annual Meeting, Nashville, USA.
- Wang, C., Jia, L., Tan, Y., et al., 2008. Carbonation of fly ash in oxy-fuel CFB combustion. *Fuel*, **87**(7):1108-1114. [doi:10.1016/j.fuel.2007.06.024]
- Watanabe, H., Yamamoto, J.I., Okazaki, K., 2011. NO<sub>x</sub> formation and reduction mechanisms in staged O<sub>2</sub>/CO<sub>2</sub> combustion. *Combustion and Flame*, **158**(7):1255-1263. [doi:10.1016/j.combustflame.2010.11.006]

## 中文概要

**题目:** 模拟富氧燃烧过程中燃料在 CO<sub>2</sub> 中稀释对 NH<sub>3</sub> 向 NO<sub>x</sub> 转化影响的研究

**目的:** 探索燃料富氧燃烧过程中不同浓度 CO<sub>2</sub> 的稀释作用对 NO<sub>x</sub> 生成的影响, 为探索 NO<sub>x</sub> 在 O<sub>2</sub>/CO<sub>2</sub> 气氛中生成机理研究提供理论基础。

**创新点:** 提出一种无分支链式反应解释说明 CO<sub>2</sub> 在还原性粒子环境中对反应的影响。

**方法:** 通过 Chemkin Pro 中塞流式反应器模块对混入 NH<sub>3</sub> 的 CH<sub>4</sub> 燃料在 O<sub>2</sub>/CO<sub>2</sub> 气氛中反应进行数值模拟, 同时改变 CO<sub>2</sub> 的稀释程度来探索 CO<sub>2</sub> 浓度对 NO<sub>x</sub> 生成的影响, 并比较不同反应机理下的模拟结果, 探索此环境中 NO<sub>x</sub> 的生成机理(表 1)。

**结论:** 1. 无支链反应机理可用于解释 CO<sub>2</sub> 在还原性粒子环境中对 NO<sub>x</sub> 生成与还原的影响; 2. 随着 CO<sub>2</sub> 浓度的升高, 无支链反应和支链反应相互竞争 H, 进而抑制 NO 的生成; 3. 在对 NH<sub>3</sub> 转化效率的影响方面, CO<sub>2</sub> 浓度增加引发的无支链反应和支链反应对 H 的竞争, 在富燃料条件下从促进转化变为抑制转化, 在化学当量和贫燃料条件下从无影响变为抑制转化。

**关键词:** CO<sub>2</sub>; 富氧燃烧; NO; 燃料稀释